ohio2/yjy-yjy/yjy-yjy/yjy99907/yjy0237d07z | xppws | 23:ver.3 | 9/25/09 | 12:10 | Msc: jp-2009-041606 | TEID: ccd00 | BATID: 00000

ORR Activity and Direct Ethanol Fuel Cell Performance of Carbon-Supported Pt−M (M = Fe, Co, and Cr) Alloys Prepared by Polyol Reduction Method

Ch. Venkateswara Rao and B. Viswanathan*

National Centre for Catalysis Research, Department of Chemistry, Indian Institute of Technology Madras, Chennai 600 036, India

Received: May 5, 2009; Revised Manuscript Received: August 25, 2009

A polyol reduction method is employed to prepare carbon-supported Pt and Pt−M (M = Fe, Co, and Cr) alloy catalysts by simultaneous reduction and decomposition of metal precursors with 1,2-hexadecanediol in the presence of nonanoic acid and nonylamine protecting agents. The prepared materials are characterized by powder XRD, HRTEM, and EDX. The face-centered cubic structure of Pt in the prepared materials is evident from XRD. Good dispersion of Pt and Pt alloy nanoparticles on the carbon support is seen from the high-resolution TEM images. The presence of respective elements with controlled composition is observed from EDX analysis. Electrochemical performance of the prepared materials is investigated by cyclic voltammetry and tested in a single-cell DEFC. The inhibition of formation of (hydr)oxy species on the Pt surface by the presence of alloying elements is observed. Oxygen reduction activity of the Pt−M/C (M = Fe, Co, and Cr) is found to be ∼1.5 times higher than that of the as-synthesized and commercial Pt/C catalysts. Single-cell DEFC tests indicated the good performance of Pt−M/C (M = Fe, Co, and Cr) compared with that of the as-synthesized and commercial Pt/C catalysts. The DEFC performance increased in the order Pt/C_{comm} < $Pt/C_{as\text{-}syn}$ < Pt−Fe/C < Pt−Co/C ∼ Pt−Cr/C. Stability under DEFC operating conditions for 50 h indicated the good stability of Pt alloys compared with that of Pt catalysts.

1. Introduction

The direct ethanol fuel cell (DEFC) is one of the alternate energy sources for transportation and portable electronic device applications. These fuel cells have received considerable attention in recent years because it uses inexpensive, abundant, less toxic and inflammable liquid ethanol as fuel.[1] The fuel cell performance and efficiency are hindered due to various limiting factors under the operating conditions. One of the issues is sluggish kinetics of the oxygen reduction reaction (ORR) at the cathode side.[2]

Even though conventional carbon-supported Pt is the efficient electrocatalyst for the ORR, it is associated with several drawbacks besides the cost issue. The main drawback is the high overpotential (0.3−0.4 V) as a result of sluggish kinetics of the ORR on the Pt surface.[3,4] To lower the overpotential, increase the oxygen reduction activity, and reduce the amount of Pt in the electrodes, significant research has been focused on platinum alloys. Pt has been alloyed with a variety of elements, including V, Cr, Ti, Mn, Fe, Co, Ni, W, Mo, Ir, Pd, and Zn. An enhancement in activity (1.5−5 times) for ORR on the alloy catalysts in comparison with pure Pt has been reported using potentiodynamic RRDE measurements.[5−21] It was also reported that the overpotential for the ORR on Pt alloys is 20−40 mV less compared to Pt. The improvement in the ORR electrocatalysis on Pt alloys has been explained by several factors, such as geometric and electronic effects.[22−27] On the basis of these investigations and in the context of the ORR mechanisms, the principle explanations for the enhanced ORR activity could be attributed to (i) modification of the electronic structure of Pt (5d-band vacancies), (ii) changes in the physical structure of Pt (Pt−Pt bond distance and coordination number), (iii) adsorption of oxygen-containing species (oxy or hydroxy species) from the electrolyte on to the Pt or alloying element, and/or (iv) redox type processes involving the first row transition alloying element. Still, what aspect of the ORR mechanism is affected by Pt−M alloy catalysts remains unclear. It is certainly true that the move toward Pt alloys as the catalyst for the ORR is necessary, but many issues still need to be resolved.

Among the various Pt bimetallic alloys, Pt−Co, Pt−Cr, and Pt−Fe appear to be good. Usually, the carbon-supported Pt alloy catalysts are prepared by the impregnation of the second metal on Pt/C and then alloying at temperatures above 973 K under reducing $Ar-H_2$ gas atmosphere.[28] The heat treatment at high temperatures gives rise to an undesired particle growth of the alloy, induces the sintering of particles, and causes the loss of surface area, which results in the decrease in specific activity for the ORR. Another issue is the change in the hydrophilic nature of the catalyst particles, making them more susceptible to flooding due to the increased hydroxide content on the surface. It is known that the particle size, dispersion, differences in surface characteristics (e.g., crystallographic plane), and compositional homogeneity of the alloy clusters resulting from the conditions employed in the synthesis procedures play an important role in the ORR catalysis. Therefore, it is of significance to prepare uniform size and shape with controllable composition of Pt−M alloys by a low-temperature chemical reduction method and investigate the ORR activity. In this context, a polyol reduction method appears to be one of the choices for the preparation of Pt bimetallic nanoparticles.[29]

The formation potential of (hydr)oxy species on the Pt surface and maximum ORR activity were found to depend significantly on the subsurface composition. Various authors reported that the bimetallic Pt−M in a 1:1, 2:1, or 3:1 ratio is optimum for good performance. Mukerjee et al.[5] reported bulk Pt−Co, Pt−Ni, and Pt−Fe alloys with an atomic ratio of 1:1 exhibited good

* Corresponding author. E-mail: bvnathan@iitm.ac.in. Tel: +91 44 2257 4241. Fax: +91 44 2257 4202.

10.1021/jp9041606 CCC: $40.75

ORR activity. According to Xiong et al.,[9] who prepared various carbon-supported Pt−M electrocatalysts by a low-temperature reduction procedure with sodium formate, reported that the Pt−Co electrocatalyst showed the best performance with the maximum catalytic activity and minimum polarization at a Pt/Co atomic ratio of around 1:7. Toda et al.[7] investigated the electrocatalytic ORR activity of Pt alloys with Co, Fe, and Ni, formed by sputtering, and observed maximum activity at ca. 40, 50, and 30% content of Co, Fe, and Ni, respectively. They also observed an increase in kinetic current densities which were 10, 15, and 20 times larger than that of pure Pt. Kinetic analysis of the data in comparison with pure Pt revealed an activity enhancement of a factor of 2−3 for the 50 atom % Co catalyst.[8] Huang et al.[18] prepared carbon-supported Pt−Co alloy catalysts with different Pt/Co atomic ratios, 1:1, 2:1, 3:1, 4:1 and 5:1, by the carbonyl complex route, followed by H_2 reduction in the temperature range of 423−573 K, and reported the maximum activity with a Pt/Co atomic ratio of 2:1. Shukla et al.[11] prepared Pt−Fe(1:1)/C by an alloying method and found the better ORR activity than that of Pt/C. Gong et al.[30] synthesized Fe-modified carbon-supported platinum electrocatalysts by a colloidal route and observed good catalytic activity at atomic compositions of Pt/Fe = 9:1 and Pt/Fe = 1:1 than the Pt/Fe = 3:1. Yang et al.[13] prepared carbon-supported Pt−Cr alloy catalysts with different Pt/Cr atomic ratios (1:1, 2:1, and 3:1) by a Pt−carbonyl route and observed the good performance in the case of Pt−Cr (1:1). Antolini et al.[31] prepared carbon-supported Pt−Cr alloy nanoparticles in 1:1, 3:1, and 9:1 atomic ratios by the $NaBH_4$ reduction method and observed good performance in the case of 1:1 and 3:1. Grinberg et al.[19] prepared carbon-supported Pt−Co and Pt−Cr alloys in a 1:1 atomic ratio by the thermal decomposition of organometallic complexes of Pt and Co or Cr and found good ORR activity than that of Pt alone. The inconsistency is due to the variation of geometric factors (degree of alloying and Pt−Pt interatomic distance) and electronic factors (Pt d-band vacancies) resulting from the preparation methods and heat treatments.

In this study, carbon-supported Pt and Pt−M (M = Fe and Co) alloy nanoparticles with an atomic ratio of 1:1 are prepared by a polyol reduction method and characterized by XRD, TEM, and EDX. Electrochemical measurements are performed to find the role of alloying elements toward the enhancement of the ORR activity. Finally, the single-cell DEFC performance of the prepared materials is investigated.

2. Experimental Section

2.1. Materials. Platinum(II) acetylacetonate, iron(II) chloride, chromium(0) hexacarbonyl, 1,2-hexadecanediol, nonanoic acid, nonylamine, Nafion solution, and polytetrafluoroethylene from Sigma-Aldrich; cobalt(0) octacarbonyl from Acros Organics; and diphenyl ether, ethyl alcohol, isopropanol, and hexane from Merck were used as received. Nafion 115 membrane was purchased from DuPont Company, U.S.A. Water purified by a Milli-Q water purification system was used throughout the experimental work. Carbon black (CDX975, received from Columbian Chemicals Company, U.S.A.) with a specific surface area (BET) of ∼300 m^2/g was used as the support for all catalysts.

2.2. Preparation of Carbon-Supported Pt−M (M = Fe, Co, and Cr) Alloy Catalysts. Uniform sized and shaped Pt−M (50:50 atom %) alloy nanoparticles are synthesized by a polyol reduction method by using platinum(II) acetylacetonate as Pt precursor; $FeCl_2$, $Co_2(CO)_8$, or $Cr(CO)_6$ as Fe, Co, or Cr, precursor, respectively; 1,2-hexadecanediol as reducing agent; and nonylamine and nonanoic acid as protecting agents. The reaction is carried out using a standard Schlenk line technique under dry nitrogen. For the preparation of carbon-supported Pt−Fe alloy nanoparticles, a mixture of 0.5 mmol of $Pt(acac)_2$, 0.5 mmol of $FeCl_2$, and 2 mmol of 1,2-hexadecanediol are taken in a 100 mL three-necked round-bottom flask equipped with a N_2 in/outlet, PTFE coated magnetic stir bar, septa rubber, and a thermal probe. Twenty-five milliliters of diphenyl ether (DPE) solvent is then transferred into the flask and the contents stirred while purging with N_2 at room temperature. The flask is then heated to 373 K and held at 373 K for 20 min. During this hold, 0.5 mmol of nonylamine and 0.5 mmol of nonanoic acid are injected into the flask while continuing the N_2 gas purge. The required amount of carbon black (C) is then added, and the dark brown suspension is heated to 523 K. The flask is maintained at the refluxing temperature of 523−533 K for 30 min before cooling to room temperature under the N_2 atmosphere. The resulting suspension is then filtered, washed copiously with ethanol, and dried at 323 K in a vacuum. Similarly, carbon-supported Pt−Co and Pt−Cr alloy catalysts are prepared. For comparison, carbon-supported Pt is also prepared. The nominal metal content on the carbon black is 20 wt %.

2.3. Characterization Techniques. X-ray diffraction (XRD) and transmission electron microscopy (TEM) are used for phase identification and determining particle size, respectively. XRD measurements are performed on a Rigaku Miniflex X-ray diffractometer using a Cu Kα source operated at 30 keV at a scan rate of 0.025° s^{-1} over the 2θ range of 10−90°. Transmission electron microscopic (TEM) images are obtained by using a high-resolution JEOL 2010 TEM system operated with an accelerating voltage of 200 kV. The sample for TEM analysis is prepared by placing a drop of dispersed catalyst onto the carbon-coated copper grid and drying in air at room temperature. An electron microscope with EDX (FEI, model Quanta 200) is used to observe the composition of the catalysts.

2.4. Electrochemical Measurements. Electrochemical performance of the catalysts is measured in both half- and full-cell modes. Half-cell measurements are performed at room temperature by cyclic voltammetry using a potentiostat (BAS 100 electrochemical analyzer). A three-electrode, one-compartment electrochemical glass cell assembled with a glassy carbon (GC) disk as the working electrode, Ag/AgCl, 3.5 M KCl (+0.205 V vs NHE) as the reference, and Pt foil as the counter electrodes, is used for the experiments. The cell containing Ar- or O_2-saturated 0.5 M H_2SO_4 is used as the electrolyte. The working electrode is fabricated as described by Schmidt et al.[32] Five milligrams of the catalyst was dispersed in 5 mL of isopropanol by ultrasonication for 20 min. The glassy carbon disk electrode (0.07 cm^2 area) was polished to a mirror finish with 0.05 μm alumina suspensions before each experiment and served as an underlying substrate of the working electrode. An aliquot of 20 μL of catalyst suspension is pipetted onto the carbon substrate. After evaporation of the isopropanol in an argon stream, the deposited catalyst is covered with 10 μL of a diluted Nafion solution (5 wt % in 15−20% water/low aliphatic alcohols) and dried at room temperature. Each electrode contained about 56 $\mu g/cm^2$ of the metal. The metal loading is found to be reproducible within ±5% based on a series of experiments in which cyclic voltammogramms are evaluated. Current densities are normalized to the geometric area of the glassy carbon substrate (0.07 cm^2). After fabrication, the electrodes are immersed in deaerated 0.5 M H_2SO_4. Owing to slight contamination from the Nafion solution, the electrode

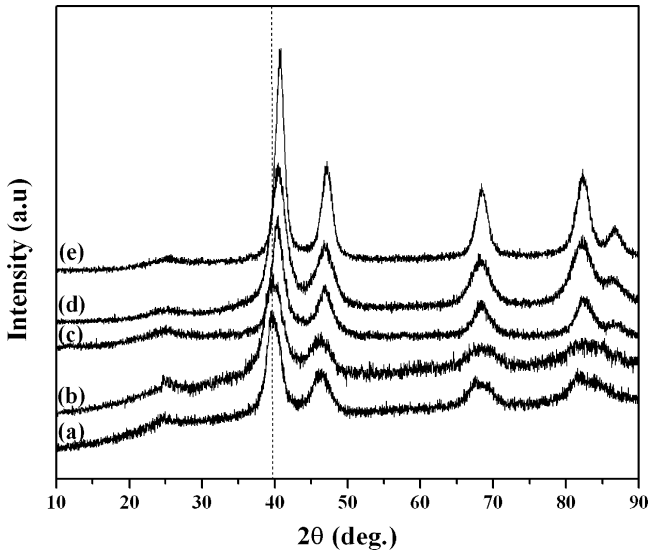

Figure 1. Powder X-ray diffraction patterns of (a) commercial Pt/C (E-TEK), (b) as-synthesized Pt/C, (c) Pt−Co(1:1)/C, (d) Pt−Cr(1:1)/C, and (e) Pt−Fe(1:1)/C catalysts.

potential is cycled 2−3 times between +0.0 and +1.0 V vs NHE in order to produce a clean electrode surface.

The measurements in full cells are obtained in a fuel cell test station. The single-cell DEFC measurements are evaluated by preparing gas diffusion electrodes. These electrodes are prepared by a combined filtration/brushing procedure using the Pt/C catalysts, a carbon cloth substrate, a PTFE suspension, and a Nafion solution. A homogeneous suspension of carbon powder, PTFE, and isoproponal was filtered under vacuum onto both faces of the carbon cloth to form the gas diffusion layer of the electrode. The amount of isopropanol used was enough to make an ink (approximately 0.5 mL for 20 mg of mass). The total mass loading for the diffusion layers of the electrodes is 3 mg/cm^2 with 15 wt % PTFE in all the cases. On top of this layer, the catalyst is applied in the form of a homogeneous suspension consisting of the required amount of the carbon-supported Pt and Pt alloy catalysts, 33 wt % Nafion and isopropanol, followed by sintering in a vacuum oven at 363 K for 1 h. The Pt metal loading is 1 mg/cm^2 for all the electrodes. The membrane−electrode assembly (MEA) is fabricated by sandwiching the Nafion 115 membrane between the cathode and anode (20 wt % Pt/C, E-TEK) by hot pressing at 398 K and 50 kg/cm^2 for 2 min. The geometric area of the electrodes is 5 cm^2. The fuel cell testing is carried out at an operating temperature of 363 K and 3 atm pressure with humidified hydrogen and oxygen gas reactants. Before the steady-state polarization curves are recorded, the cell was kept at a constant current density of 20 mA/cm^2 for 2 h until the open circuit voltage (OCV) became steady and constant (MEA conditioning). The polarization curve is then recorded by applying potential from 0.7 to 0.0 V. A commercial sample of 20 wt % platinum on carbon (E-TEK) is also examined for comparison.

3. Results and Discussion

F1 **3.1. XRD Analysis.** Figure 1 shows the XRD patterns of the carbon-supported Pt and Pt−M (50:50 atom %) alloy catalysts and commercial Pt/C (E-TEK) recorded in the 2θ range of 10−90°. As indicated in Figure 1, all the catalysts exhibited five characteristic diffraction peaks at 2θ values around 40, 47, 68, 82 and 87°, corresponding to the (111), (200), (220), (311), and (222) planes of the face-centered cubic (fcc) structure of Pt (JCPDS no. 87-0640). In the case of Pt−M/C catalysts, diffraction peaks are shifted to higher 2θ values with respect to the corresponding peaks in the as-synthesized and commercial Pt/C catalysts. It indicates the contraction of the lattice by the incorporation of base metal (Fe, Co, or Cr) in the fcc structure of Pt due to the alloy formation. This shift also suggests that the interatomic distance of Pt is decreased due to the substitution of a smaller atom, such as a transition-metal, Fe, Co, or Cr.[8,33] The interatomic Pt−Pt distance in commercial Pt/C, as-synthesized Pt/C, Pt−Fe/C, Pt−Co/C, and Pt−Cr/C catalysts are calculated to be 2.77, 2.77, 2.73, 2.73, and 2.72, respectively. No peaks for pure the base metal or its oxides are observed, but their presence cannot be discarded because they may be present in a small amount or even in an amorphous form. The broad peak observed at around 2θ = 24−26° is due to the hexagonal structure of the carbon support. It is known that oxygen is adsorbed on the Pt surface by dual site mode; therefore, the Pt−Pt nearest-neighbor distance plays the key role in determining the adsorption behavior. Jalan and Taylor[22] have studied the effect of the Pt−Pt nearest-neighbor distance and oxygen reduction activity of various platinum alloys. They claimed that the short Pt−Pt nearest-neighbor distance in alloys compared with that of the pure Pt causes the facile reduction of oxygen. Literature reports also indicate that the best electrocatalytic activity for the ORR is observed when the Pt−Pt interatomic distance is 0.273−0.274 nm.[7,26] The compressed Pt−Pt bond length has shown to lower the valence band center relative to the Fermi level,[34−36] reduce the binding strength and/or coverage of oxygenated adsorbates,[6,26] and enhance ORR activity. The contraction of the Pt lattice observed in the case of as-prepared Pt−M/C alloy catalysts may be favorable for dissociation of oxygen and enhance the kinetics.

F2 **3.2. TEM and EDX Analysis.** Figure 2 shows the TEM image and the corresponding EDX of the carbon-supported Pt and Pt−M alloy catalysts. A good spatial distribution of spherically shaped particles over the carbon support with a narrow particle size distribution is observed. The mean particle diameter (d) is calculated by using the formula $d = (\sum_i n_i d_i)/(n_i)$, where n_i is the frequency of occurrence of particles of the size d_i. TEM analysis reveals the mean diameter of 3.8, 5, 5, and 6.5 nm with a standard deviation of 0.1−0.2 for the carbon-supported Pt, Pt−Co, Pt−Cr, and Pt−Fe catalysts, respectively (Table 1). EDX spectra of the carbon-supported Pt and Pt−M alloy catalysts confirm the presence of respective elements and a small amount of oxygen. The average composition of elements in the Pt−M alloy catalysts by the collection of data for 50 nanoparticles is found to be approximately 1:1 (Table 1). T1

F3 **3.3. Electrochemical Performance of the Catalysts.** Figure 3 shows the cyclic voltammograms of carbon-supported Pt and Pt−M (M = Fe, Co, and Cr) alloys and commercial Pt/C (E-TEK) catalysts in deaerated 0.5 M H_2SO_4 at the scan rate of 25 mV/s. In the case of Pt/C catalysts, well-defined reversible hydrogen desorption/adsorption peaks and irreversible preoxidation/reduction peaks are observed. During the anodic scan, hydrogen is desorbed between −0.05 and +0.3 V vs NHE and surface platinum oxides are formed beyond +0.8 V vs NHE. During the cathodic scan, the surface platinum oxides are reduced between +1.0 and +0.5 V vs NHE and hydrogen is adsorbed at potentials more cathodic than +0.3 V vs NHE. It is thought that, in acid solution, OH_{ads} is formed from oxidation of water on platinum surfaces at around +0.8 V and blocks surface sites for O_2 adsorption, thus resulting in low ORR activity.[37] However, no well-defined hydrogen adsorption/desorption peaks on the carbon-supported Pt−M alloy catalysts

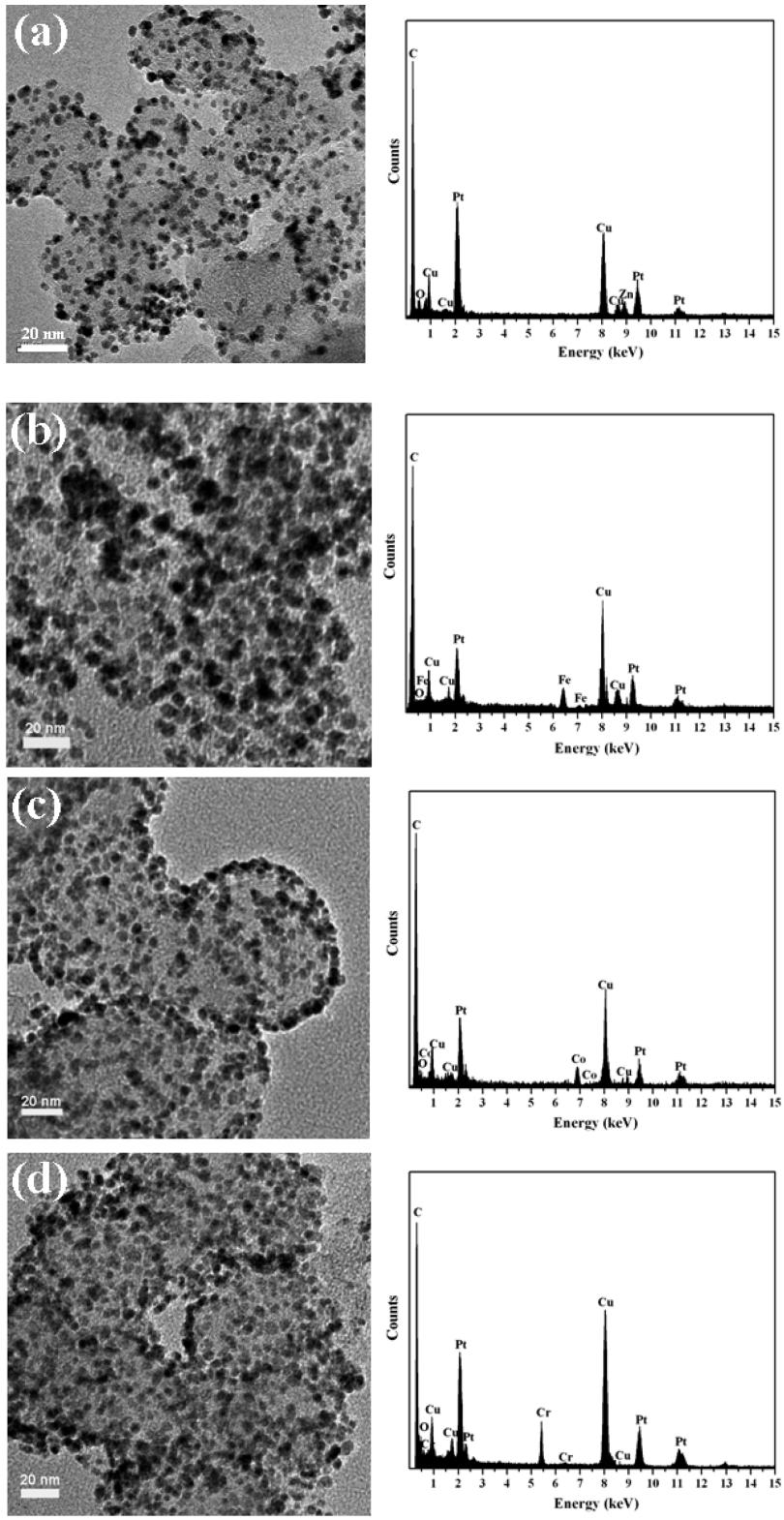

Figure 2. TEM images (left) and corresponding EDX spectrum (right) of carbon-supported Pt and Pt alloy catalysts prepared by a polyol reduction method: (a) Pt/C, (b) Pt−Fe(1:1)/C, (c) Pt−Co(1:1)/C, and (d) Pt−Cr(1:1)/C.

is observed, suggesting the high dispersion of the catalysts with the disordered surface structure. The electrochemically active surface area (EAS) evaluated from the hydrogen adsorption/desorption peaks is calculated to be 75, 72, 55, 56, and 43 m^2/g for Pt/C (commercial), Pt/C (as-syn), Pt−Co/C, Pt−Cr/C, and Pt−Fe/C catalysts, respectively.

A comparison of the voltammetry of carbon-supported Pt and Pt−M alloy catalysts shows the difference in the onset of oxide formation on Pt (accepted as Pt−OH). Pt−M/C catalysts exhibit a significantly lower extent of oxide formation than that of Pt/C catalysts. The inhibition of formation of $-OH_{ads}$ species over Pt−M/C catalysts is due to the d-orbital coupling between the low occupancy of d orbitals in Fe, Co, or Cr and high occupancy of d orbitals in Pt, which leads to the decrease of the DOS at the Fermi level of Pt and down shift of the Pt d-band center energy. The foreign atoms in the Pt−M alloys behave as electron

TABLE 1: Elemental Composition, Particle Size, Onset Potential for Oxygen Reduction, and ORR Activity of Carbon-Supported Pt and Pt−M (M = Fe, Co, and Cr) Alloys Prepared by a Polyol Reduction Method and Commercial Pt/C Catalysts

catalyst	elemental composition by EDX (atom %) (Pt/M)	particle size (nm)	onset potential for oxygen reduction (mV vs NHE)	ORR activity at +0.7 V vs NHE (mA/cm^2)	single-cell DEFC performance (mW/cm^2)
Pt/C (E-TEK)	100:0	3.7 ± 0.4	+915	3.1	7
Pt/C (as-syn)	100:0	3.8 ± 0.2	+925	3.4	10
Pt−Fe(1:1)/C	51:49	6.5 ± 0.2	+955	4.2	16
Pt−Co(1:1)/C	50:50	5.0 ± 0.1	+980	5.0	20
Pt−Cr(1:1)/C	48:52	5.0 ± 0.2	+985	5.1	21

donors to the Pt atom; thus, Pt becomes negatively charged and foreign elements become positively charged. As a result, it causes the strong interaction of foreign elements with the negatively charged O of the adsorbed hydroxy ($-OH_{ads}$) species. The binding energies of O, OH, and H_2O to bimetallic clusters PtX, PtPtX, and PtXX (X is the foreign atom like Co and Cr), calculated by DFT calculations, also show that the second metal element in the alloy has a stronger affinity for OH, O, and H_2O than the Pt sites.[38] The decreased DOS at the Fermi level of Pt by the electron transfer from Fe, Co, or Cr to Pt also weakens the chemisorption bonds between Pt and the adsorbed species, thereby reducing their blocking effect in the oxygen-reduction process. Downshift of the Pt d-band center (relative to the Fermi level, which determines the surface reactivity), in the case of Pt−M alloys, causes the shift of OH_{ads} formation over Pt−M alloy catalysts. As a result, the OH_{ads} formation was observed at +0.8 V vs NHE in the case of Pt/C catalysts and around +0.85 vs NHE in the case of Pt−M (M = Fe, Co, and Cr) alloys. These results indicate that the alloying of Pt with a base metal inhibits the chemisorption of (hydr)oxy species on the Pt sites at high potentials (above +0.8 V) by the change in electronic structure. This may have a beneficial effect on the oxygen adsorption at low overpotential and thus may lead to an enhancement of the ORR kinetics.[26,37]

Figure 4 shows the linear sweep voltammograms (LSVs) of carbon-supported Pt and Pt−M (M = Fe, Co, and Cr) alloys and commercial Pt/C (E-TEK) catalysts in Ar- and O_2-saturated 0.5 M H_2SO_4 between +0.2 and +1.2 V vs NHE at a scan rate of 5 mV/s. It is evident that the oxygen reduction on all the catalysts is diffusion-controlled when the potential is less than +0.7 V and is under mixed diffusion-kinetic control in the potential region between +0.7 and +1.0 V vs NHE. For all catalysts, when the potential was swept from +1.2 to +0.2 V, a single oxygen reduction peak is observed in the potential region of ca. 1.0−0.7 V. The steep increase in peak current at +0.7 V indicates the facile kinetics of the ORR. Oxygen reduction activity of the catalysts is calculated by taking the difference in activity at +0.7 V vs NHE in Ar- and O_2-saturated 0.5 M H_2SO_4 and given in Table 1. The results of linear sweep voltammetry indicate that the Pt−M/C (M = Fe, Co, and Cr) catalysts exhibited 1.5−1.7 times higher ORR activity than the Pt/C catalysts. The high ORR activity is attributed to the inhibition of formation of (hydr)oxy species on the Pt surface. Among the investigated Pt−M/C catalysts (M = Fe, Co, and Cr), maximum ORR activity is observed for the Pt−Cr(1:1)/C and Pt−Co(1:1)/C. Moreover, oxygen reduction proceeded in a relatively positive potential region for the Pt−M/C (M = Fe, Co, and Cr) catalysts compared to the Pt/C. The overpotential for the ORR of the Pt alloys is about 40−70 mV less compared with that of Pt (Table 1). This may be due to differences in the surface activation, which is related to the size and distribution of the metallic nanoparticles. The similar shape of LSVs and high current density of Pt alloy catalysts to that of the Pt/C catalyst indicate that the oxygen reduction takes place in the same manner on the catalysts but with facile kinetics on Pt alloys. These results are in good agreement with the EXAFS

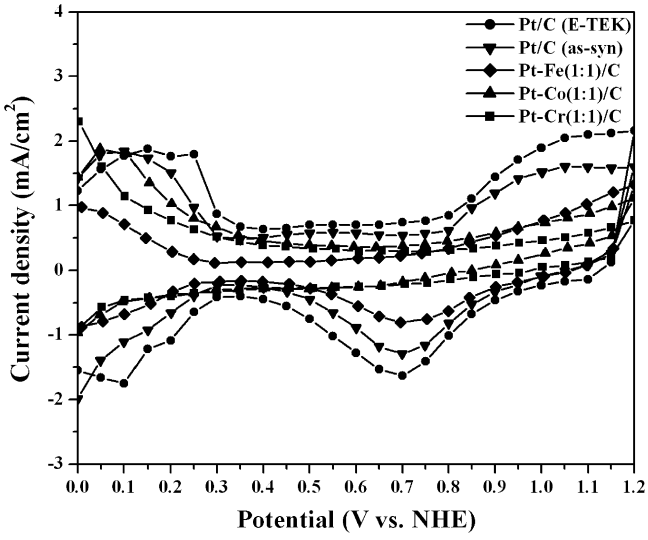

Figure 3. Cyclic voltammograms (CVs) of carbon-supported Pt and Pt−M (M = Fe, Co, and Cr) alloys prepared by a polyol reduction method and commercial Pt/C (E-TEK) catalysts in Ar-saturated 0.5 M H_2SO_4. Scan rate = 25 mV/s.

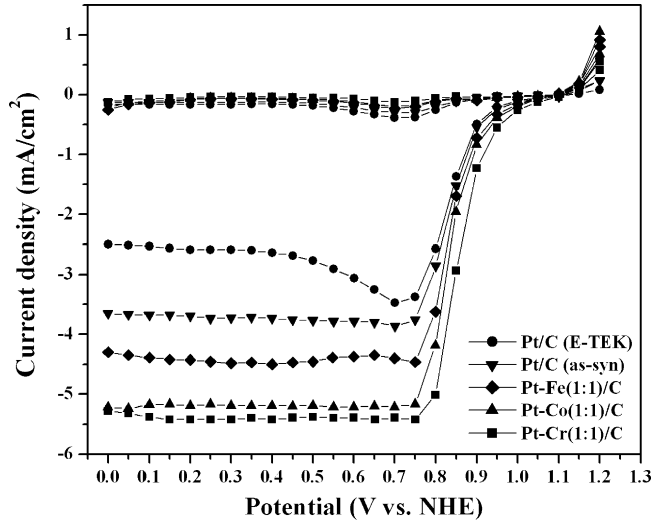

Figure 4. Linear sweep voltammograms (LSVs) of carbon-supported Pt and Pt−M (M = Fe, Co, and Cr) alloys prepared by a polyol reduction method and commercial Pt/C (E-TEK) catalysts in Ar- and O_2-saturated 0.5 M H_2SO_4. Scan rate = 5 mV/s (empty and full symbols corresponding to the LSVs in Ar- and O_2-saturated 0.5 M H_2SO_4, respectively).

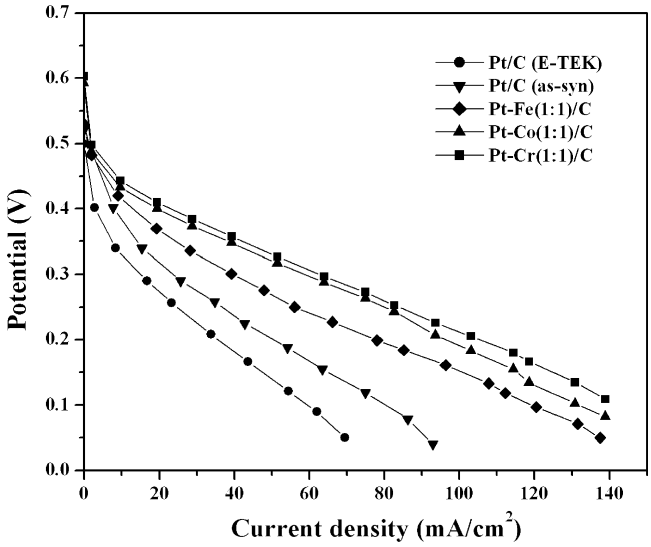

Figure 5. Single-cell DEFC polarization curves with carbon-supported Pt and Pt−M (M = Fe, Co, and Cr) alloys prepared by a polyol reduction method and commercial Pt/C (E-TEK) electrocatalysts for oxygen reduction at 363 K and 3 atm using 1 M ethanol solution. Cathode: Pt loading = 1 mg/cm^2. Anode: 20 wt % Pt/C, Pt loading = 1 mg/cm^2.

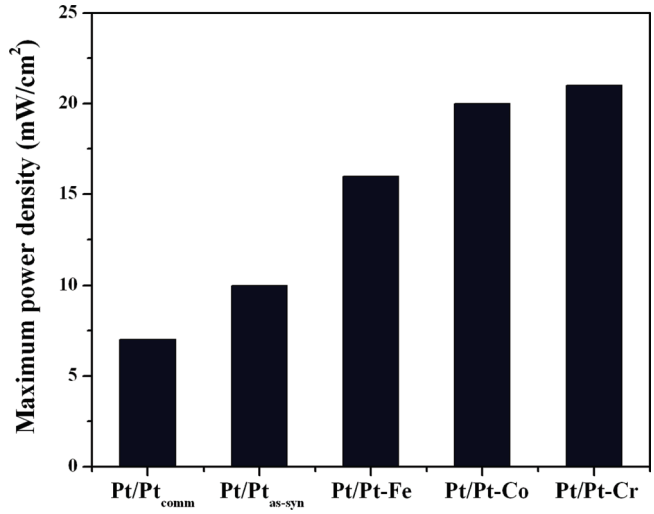

Figure 6. Histograms of the maximum power density of DEFCs operating at 363 K and 3 atm with carbon-supported electrocatalysts: Pt (commercial), Pt (as-synthesized), Pt−Fe, Pt−Co, and Pt−Cr as cathode and Pt as anode.

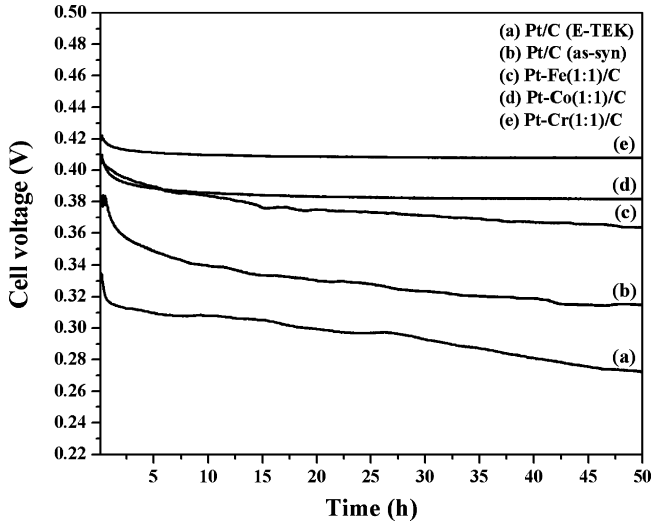

Figure 7. Cell voltage−time curves of carbon-supported Pt and Pt−M (M = Fe, Co, and Cr) alloys prepared by a polyol reduction method and commercial Pt/C (E-TEK) electrocatalysts for oxygen reduction in single-cell DEFCs at 10 mA/cm^2 for 50 h.

measurements performed by Mukerjee et al.[26] and ORR measurements on bulk Pt alloys performed by Toda et al.[7]

Single-cell DEFC performance and stability of the electrocatalysts are important evaluation criteria for practical applications. Figure 5 compares the electrochemical performances in a single-cell DEFC using the carbon-supported Pt and Pt−M (M = Fe, Co, and Cr) alloys and the commercial Pt/C (E-TEK) catalyst with the same metal loading as the cathode under the identical testing conditions. The as-synthesized Pt−M/C (M = Cr, Co, and Fe) catalysts exhibited better performance with low polarization losses at both low and high current densities than that of Pt/C catalysts. At 0.4 V, carbon-supported Pt−Fe, Pt−Co, and Pt−Cr catalysts yielded a current density of 13.2, 18.9, and 21.4 mA/cm^2, whereas the as-synthesized and commercial Pt/C catalysts yielded 7.7 and 3.3 mA/cm^2, respectively. Moreover, carbon-supported Pt−Fe, Pt−Co, and Pt−Cr catalysts show an open circuit voltage of 0.53, 0.59, and 0.61 V, respectively, which is higher than that found with the as-synthesized and commercial Pt/C catalysts (0.5 V). The values of the maximum power density (MPD) of single-cell DEFCs at 363 K and 3 atm are reported in Figure 6. The increase in power density in going from Pt (7−10 mW/cm^2) to Pt−M alloys (16, 20, and 21 mW/cm^2 for Pt−Fe, Pt−Co, and Pt−Cr, respectively) as cathode material is observed. The improvement of DEFC performance of Pt−M alloys is due to the alloying effect. Figure 7 shows the cell voltage−time curves of the catalysts recorded at 10 mA/cm^2 for 50 h under identical DEFC conditions. The cell with the Pt−M/C (M = Fe, Co, and Cr) alloys as cathodes exhibited stable voltage with low polarization losses, whereas the as-synthesized and commercial Pt/C catalysts exhibited significantly high polarization losses within the period of 50 h. Among all the investigated catalysts, carbon-supported Pt−Co and Pt−Cr exhibited good performance.

4. Conclusions

Carbon-supported Pt and Pt−M alloy (M = Fe, Co, and Cr) nanoparticles are prepared by a polyol reduction method and characterized by XRD, TEM, and EDX. Spherically shaped nanoparticles with a narrow size distribution are observed on a carbon support. Electrochemical measurements indicate that the Pt alloys exhibited an ∼1.5 times higher ORR activity and ∼50 mV lower overpotential than that of Pt/C catalysts. The enhanced ORR activity is due to the inhibition of formation of (hydr)oxy species on the Pt surface by the presence of alloying elements. Single-cell DEFC tests showed the good performance of Pt alloys compared with that of the Pt/C catalysts. The high ORR activity, low overpotential, good single-cell DEFC performance, and stability of the Pt−M/C (M = Fe, Co, and Cr) compared with that of as-synthesized and commercial Pt/C make them more appropriate cathodes for DEFC applications.

Acknowledgment. The authors wish to acknowledge Columbian Chemicals Company, U.S.A., for financial support and also the Department of Science and Technology (DST), India, for creating the National Centre for Catalysis Research at IIT Madras.

References and Notes

(1) Arico, A. S.; Creti, P.; Antonucci, P. L.; Antonuccci, V. *Electrochem. Solid-State Lett.* **1998**, *1*, 66.

(2) Lamy, C.; Lima, A.; Lerhun, V.; Delime, F.; Coutanceau, C.; Léger, J.-M. *J. Power Sources* **2002**, *105*, 283.
(3) Ralph, T. R.; Hogarth, M. P. *Platinum Met. Rev.* **2002**, *46*, 3.
(4) Gasteiger, H. A.; Shyam, S. K.; Sompalli, B.; Wagner, F. T. *Appl. Catal., B* **2005**, *56*, 9.
(5) Mukerjee, S.; Srinivasan, S. *J. Electroanal. Chem.* **1993**, *357*, 201.
(6) Mukerjee, S.; Srinivasan, S.; Soriaga, M. P.; McBreen, J. *J. Phys. Chem.* **1995**, *99*, 4577.
(7) Toda, T.; Igarashi, H.; Uchida, H.; Watanabe, M. *J. Electrochem. Soc.* **1999**, *146*, 3750.
(8) Paulus, U. A.; Wokaun, A.; Scherer, G. G.; Schmidt, T. J.; Stamenkovic, V.; Radmilovic, V.; Markovic, N. M.; Ross, P. N. *J. Phys. Chem. B* **2002**, *106*, 4181.
(9) Xiong, L.; Kannan, A. M.; Manthiram, A. *Electrochem. Commun.* **2002**, *4*, 898.
(10) Antolini, E.; Passos, R. R.; Ticianelli, E. A. *Electrochim. Acta* **2002**, *48*, 263.
(11) Shukla, A. K.; Raman, R. K.; Choudhury, N. A.; Priolkar, K. R.; Sarode, P. R.; Emura, S.; Kumashiro, R. *J. Electroanal. Chem.* **2004**, *563*, 181.
(12) Yang, H.; Vogel, W.; Lamy, C.; Alonso-Vante, N. *J. Phys. Chem. B* **2004**, *108*, 11024.
(13) Yang, H.; Alonso-Vante, N.; Lèger, J.-M.; Lamy, C. *J. Phys. Chem. B* **2004**, *108*, 1938.
(14) Li, W.; Zhou, W.; Li, H.; Zhou, Z.; Zhou, B.; Sun, G.; Xin, Q. *Electrochim. Acta* **2004**, *49*, 1045.
(15) Antolini, E.; Salgado, J. R. C.; Santos, L. G. R. A.; Garcia, G.; Ticianelli, E. A.; Pastor, E.; Gonzalez, E. R. *J. Appl. Electrochem.* **2006**, *36*, 355.
(16) Ioroi, T.; Yasuda, K. *J. Electrochem. Soc.* **2005**, *152*, A1917.
(17) Sode, A.; Li, W.; Yang, Y.; Wong, P. C.; Gyenge, E.; Mitchell, K. A. R.; Bizzotto, D. *J. Phys. Chem. B* **2006**, *110*, 8715.
(18) Huang, Q.; Yang, H.; Tang, Y.; Lu, T.; Akins, D. L. *Electrochem. Commun.* **2006**, *8*, 220.
(19) Grinberg, V. A.; Kulova, T. L.; Maiorova, N. A.; Dobrokhotova, Zh. V.; Pasynskii, A. A.; Skundin, A. M.; Khazova, O. A. *Russ. J. Electrochem.* **2007**, *43*, 75.
(20) Li, H.; Sun, G.; Li, N.; Sun, S.; Su, D.; Xin, Q. *J. Phys. Chem. C* **2007**, *111*, 5605.
(21) Qian, Y.; Wen, W.; Adcock, P. A.; Jiang, Z.; Hakim, N.; Saha, N.; Mukerjee, S. *J. Phys. Chem. C* **2008**, *112*, 1146.
(22) Jalan, V.; Taylor, E. J. *J. Electrochem. Soc.* **1983**, *130*, 2299.
(23) Paffet, M. T.; Beery, G. J.; Gottesfeld, S. *J. Electrochem. Soc.* **1988**, *135*, 1431.
(24) Beard, B. C.; Ross, P. N. *J. Electrochem. Soc.* **1990**, *137*, 3368.
(25) Watanabe, M.; Tsurumi, K.; Mizukami, T.; Nakamura, T.; Stonehart, P. *J. Electrochem. Soc.* **1994**, *141*, 2659.
(26) Mukerjee, S.; Srinivasan, S.; Soriaga, M. P.; McBreen, J. *J. Electrochem. Soc.* **1995**, *142*, 1409.
(27) Antolini, E.; Salgado, J. R. C.; Giz, M. J.; Gonzalez, E. R. *Int. J. Hydrogen Energy* **2005**, *30*, 1213.
(28) Salgado, J. R. C.; Antolini, E.; Gonzalez, E. R. *Appl. Catal., B* **2005**, *57*, 283.
(29) Sun, S.; Murray, C. B.; Weller, D.; Folks, L.; Moser, A. *Science* **2000**, *287*, 1989.
(30) Gong, Y.; Yeboah, Y. D.; Lvov, S. N.; Balashov, V.; Wang, Z. *J. Electrochem. Soc.* **2007**, *154*, B560.
(31) Antolini, E.; Salgado, J. R. C.; Santos, L. G. R. A.; Garcia, G.; Ticianelli, E. A.; Pastor, E.; Gonzalez, E. R. *J. Appl. Electrochem.* **2006**, *36*, 355.
(32) Schmidt, T. J.; Gasteiger, H. A.; Stab, G. D.; Urban, P. M.; Kolb, D. M.; Behm, R. J. *J. Electrochem. Soc.* **1998**, *145*, 2354.
(33) Hwang, J. T.; Chung, J. S. *Electrochim. Acta* **1993**, *38*, 2715.
(34) Xu, Y.; Ruban, A. V.; Mavrikakis, M. *J. Am. Chem. Soc.* **2004**, *126*, 4717.
(35) Mavrikakis, M.; Hammer, B.; Norskov, J. K. *Phys. Rev. Lett.* **1998**, *81*, 2819.
(36) Grabow, L.; Xu, Y.; Mavrikakis, M. *Phys. Chem. Chem. Phys.* **2006**, *8*, 3369.
(37) Murthi, V. S.; Urian, R. C.; Mukerjee, S. *J. Phys. Chem. B* **2004**, *108*, 11011.
(38) Balbuena, P. B.; Altomare, D.; Vadlamani, N.; Bingi, S.; Agapito, L. A.; Seminario, J. M. *J. Phys. Chem. B* **2004**, *108*, 6378.

JP9041606